European Journal of Pharmacology 1026 (2026) 178960

Contents lists available at ScienceDirect

European Journal of Pharmacology

journal homepage: www.elsevier.com/locate/ejphar

SAHA induces immunogenic cell death in triple negative breast cancer cells and its efficacy is enhanced by SOCS3 functional replacement

Giuliano Castellano [a,1], Candida Bucciero [a,1], Alessia Cugudda [b], Sara La Manna [b], Daniela Marasco [b], Giuseppe Portella [a], Anna Maria Malfitano [a,*]

[a] Department of Translational Medical Sciences, University of Naples Federico II, Naples, 80131, Italy
[b] Department of Pharmacy, University of Naples Federico II, Naples, 80131, Italy

ARTICLE INFO

Keywords:
SAHA
HDACIs
TNBC
Immunogenic cell death (ICD)
SOCS3
STAT3

ABSTRACT

Triple negative breast cancer (TNBC) is an aggressive subtype associated with poor prognosis and limited therapeutic options. Epigenetic changes contribute to TNBC tumorigenesis, and histone deacetylase inhibitors (HDACi) have emerged as promising therapeutic agents. However, their efficacy as monotherapy in solid tumors remains limited. Recent evidence highlights their immunomodulatory potential, supporting the development of combination strategies. We investigated the effect of the HDACi suberoylanilide hydroxamic acid (SAHA) on cell viability and immunogenic cell death (ICD), as well as its combinatory potential with a SOCS3 peptidomimetic (KIRCONG chim PEG), designed to inhibit STAT3 phosphorylation (pSTAT3), in TNBC cell lines. SAHA reduced TNBC cell viability and, at its IC_{25}, induced ICD hallmarks in MDA-MB-231 cells, including ATP release, calreticulin surface exposure, and increased HMGB1 levels, accompanied by enhanced IL-6 secretion. In contrast, MDA-MB-468 cells showed limited ICD features under the same conditions. The higher IL-6 secretion observed in untreated MDA-MB-231 cells was associated with lower basal SOCS3 expression compared to MDA-MB-468 cells. Given the potential role of IL-6/JAK/STAT3 signaling in limiting HDACi efficacy, SAHA was combined with the SOCS3 peptidomimetic KIRCONG chim PEG. In MDA-MB-231 cells, co-treatment reduced pSTAT3 levels and increased BAK expression. Moreover, the combination shifted the IC_{25} of SAHA, indicating enhanced sensitivity to sub-toxic concentrations. Conditioned media from co-treated MDA-MB-231 cells promoted $CD4^+$T cell activation, as shown by increased HLA-DR and CD69 expression. Overall, these findings indicate that SOCS3 functional replacement enhances SAHA anti-cancer and immunogenic effects in IL-6 high TNBC cells, supporting a context-dependent combinatory strategy targeting the IL-6/STAT3 axis.

1. Introduction

Triple negative breast cancer (TNBC) is a breast cancer (BC) subtype characterized by highly metastatic profile lacking estrogen receptor (ER), progesterone receptor (PR), and human epidermal growth factor receptor 2 (HER2/neu or ERBB2) (Bianchini et al., 2022). Among the epigenetic modifications, histone acetylation and deacetylation play a pivotal role in TNBC progression. Histone deacetylases (HDACs) promote chromatin condensation and transcriptional reprogramming through the deacetylation of histone (H3 and H4) and non-histone proteins including p53, Hsp90, PTEN, and tubulin. As Zn^{2+} or NAD^+-dependent enzymes, HDACs contribute to abnormal cell proliferation favoring invasion, stemness, angiogenesis and metastatic diffusion in TNBC (Nimal et al., 2024).

In this context, HDAC inhibitors (HDACi) have emerged as promising therapeutic agents capable of reversing cancer-associated epigenetic abnormalities (Bolden et al., 2013; Göttlicher et al., 2001). Epigenetic therapy with HDACi has demonstrated immune-modulatory effects (Medon et al., 2017), including enhanced natural killer (NK) cell-mediated cytotoxicity (Shen et al., 2017), increased trastuzumab-dependent phagocytosis in HER2+ BC cells (Laengle et al., 2020) and improved T-cell mediated lysis of TNBC cells in vitro (Gameiro et al., 2016). To date, several HDACi have gained FDA approval for cancer treatment (He et al., 2001), including vorinostat (suberoylanilide hydroxamic acid, SAHA), an inhibitor of class I and II HDACs approved for treatment of cutaneous T-cell lymphoma (Mann

* Corresponding author.
E-mail address: annamaria.malfitano@unina.it (A.M. Malfitano).
[1] These authors contributed equally to this work.

https://doi.org/10.1016/j.ejphar.2026.178960
Received 1 September 2025; Received in revised form 30 April 2026; Accepted 8 May 2026
Available online 8 May 2026

et al., 2007).

Despite their efficacy in hematological malignancies, HDACi have shown limited success as single agents in solid tumors including breast, renal, and prostate cancers (Kelly et al., 2005; Giannini et al., 2012). Consequently, combinatory approaches targeting complementary pathways have gained increasing interest. In TNBC models, SAHA combined with immune checkpoint inhibitors (Terranova-Barberio et al., 2017), leukemia inhibitory factor receptor (LIFRα) inhibitor EC359 (Li et al., 2021), or G-quadruplex stabilizing agents (Jiang et al., 2022) has demonstrated enhanced anti-cancer activity. Additional combinations, including SAHA with eribulin (Oba et al., 2021), olaparib (Min et al., 2015), the lysine-specific demethylase 1 (LSD1) inhibitor pargyline (Vasilatos et al., 2013), or apigenin (Nimal et al., 2024), further improved therapeutic efficacy. SAHA has also been shown to enhance radiosensitivity in TNBC human and murine cells by reducing lung metastasis (Chiu et al., 2013).

Emerging evidence indicates that persistent STAT3 activation may limit HDACi efficacy in solid tumors. Hybrid molecules like Roxyl-zhc-84 combining pharmacophoric elements for HDACs and cyclin-dependent kinases (CDK) have been shown to overcome JAK1-STAT3-BCL2-mediated drug resistance, increasing apoptosis in TNBC cells (Huang et al., 2018). Similarly, dual JAK/HDACi exhibited potent anti-proliferative and pro-apoptotic effects in TNBC models through suppression of phosphorylated STAT3 (pSTAT3) and downregulation of the LIFR-JAK-STAT signaling pathway (Liang et al., 2022). Suppressors of cytokine signaling 3 (SOCS3) acts as endogenous negative regulators of IL-6–mediated JAK/STAT signaling. Peptidomimetics of SOCS3 have been developed to inhibit IL-6-induced pSTAT3 activation in cancer. Notably, the chimeric SOCS3 peptidomimetic KIRCONG chim PEG, bearing a polyethylene glycol (PEG) moiety, has been shown to selectively penetrate TNBC cells and reduce pSTAT3 levels and transcriptional activity (La Manna et al., 2024).

In this study we investigated the effect of SAHA in TNBC cells focusing on its ability to induce immunogenic cell death (ICD) and evaluating its anti-cancer potential in combination with the SOCS3 peptidomimetic KIRCONG chim PEG.

2. Material and methods

2.1. Cells and drugs

TNBC cells (MDA-MB-231 and MDA-MB-468 cell lines) were cultured in Dulbecco's Modified Eagle Medium (DMEM, GIBCO, Paisley, UK). DU4475 cells were cultured in Roswell Park Memorial Institute Medium (RPMI-1640, GIBCO, Paisley, UK). Human peripheral blood mononuclear cells (PBMCs) were isolated from healthy female donors by Lymphosep (AU-L0560-500, Aurogene) over density gradient centrifugation and cultured in RPMI-1640. Growth media were supplemented with 2 mM L-glutamine, 50 ng/mL, streptomycin, 50 units/mL penicillin, and 10% heat-inactivated fetal bovine serum (FBS, GIBCO). Cells were maintained in a humidified atmosphere with 5% CO2 at 37 °C and harvested upon reaching 70–80% of confluence with 0.25% trypsin (Sigma-Aldrich, St Louis, MO, USA). Suberoylanilide Hydroxamic Acid (SAHA, Vorinostat, Merck) was dissolved in dimethyl sulfoxide (DMSO, Sigma Aldrich). The SOCS3 peptidomimetic, KIRCONG chim PEG, conjugated to the cell penetrating peptide (CPP)-Tat (48–60 fragment of HIV Tat protein) was synthesized according to previously described procedures (La Manna et al., 2024) and dissolved in H_2O.

2.2. 3-[4,5-Dimethylthiazol-2-yl]-2,5-diphenyl tetrazolium bromide (MTT) assays

MTT viability assay was performed in TNBC cell lines following treatment with increasing concentrations of SAHA. MDA-MB-231 (1000 cells/well), MDA-MB-468 (1500 cells/well) and DU4475 (1500 cells/well) cells were seeded in triplicates in 96-wellplate and allowed to adhere overnight.

For combination experiments, cells were treated with different concentrations of SAHA in the presence or absence of KIRCONG chim PEG (15 μM). After 72h of incubation, 10 μl of MTT solution (Sigma) were added to each well during the final 4 h of incubation. DMSO was added to each well to dissolve the formazan crystals and absorbance was measured within 1 h at 570 nm by Glomax Discover Microplate Reader (Promega, Madison, WI, USA) as previously described (Florio et al., 2019; La Manna et al., 2023). IC_{25} and IC_{50} values were calculated using GraphPad Prism version 10.4.

2.3. Extracellular adenosine triphosphate (ATP) release

MDA-MB-231 (1000 cells/well) and MDA-MB-468 (1500 cells/well) were seeded in duplicates in 96-well plates and allowed to adhere. Cells were then treated with SAHA at the concentration of 0.2 μM (IC_{25}) for 72h. After the incubation, cell supernatants were collected and processed to evaluate extracellular ATP release according to manufacturing instructions of ATPlite Luminescence Assay System (PerkinElmer, MA, USA). Luminescence was measured as an indicator of extracellular ATP, as the emitted light signal is directly proportional to ATP concentration.

2.4. Calreticulin (CALR) evaluation

To detect CALR on cell surface, MDA-MB-231 ($6x10^4$ cells) and MDA-MB-468 ($4x10^4$ cells) were seeded in 6-well plates and treated with SAHA at IC_{25} for 72h. After the incubation, cells were detached with trypsin, collected, washed with PBS, and stained with calreticulin-PE conjugated antibody (1:100, Enzo Life Sciences, New York, NY, USA) for 15 min on ice as previously described (Di Somma et al., 2019a). After the staining, cells were washed with PBS and analyzed by flow cytometry. Data acquisition was performed with a BD LSRFortessa (BD Biosciences, San Jose, CA, USA) and analyses were carried out using Flowlogic Software (MACS, Miltenyi Biotec).

2.5. High mobility group box 1 (HMGB1) intracellular amount and extracellular release

MDA-MB-231 ($6x10^4$ cells) and MDA-MB-468 ($4x10^4$ cells) were seeded in 6-well plates and left to adhere overnight. Cells were then treated with SAHA at the IC25 for 72h. After the incubation, cells were detached with trypsin, washed with PBS, permeabilized in methanol (90%) for 10 min on ice, and stored at −20 °C prior to intracellular staining to evaluate HMGB1 levels. Cells were then washed and re-suspended in FACS buffer (BSA 0.2%, NaN_3 0.05% in PBS), incubated with HMGB1-PE conjugated antibody (BioLegend) for 30 min at room temperature (R.T.), washed in PBS, re-suspended in FACS buffer and analyzed by flow cytometry.

To detect extracellular HMGB1 release, MDA-MB-231 cells (5×10^5 cells per 60-mm culture dish) were seeded and allowed to adhere overnight, followed by serum starvation overnight. Cells were then treated with SAHA at the IC_{25} for 24h. Cell culture supernatants were collected and analyzed according to manufacturer's instructions using a Human HMGB-1 ELISA Kit (Elabscience, E-EL-H1554).

2.6. ELISA assays

To assess IL-6 and IL-8 production, TNBC cells (1×10^6) were seeded in 12-well-plates. After 12h of adherence, cells were serum-starved for 24 h and then treated with SAHA at IC_{25} for 24h. Cell culture supernatants were collected and centrifuged at 1600 rpm for 5 min at R.T. to remove cell debris. IL-6 and IL-8 levels were quantified by ELISA according to manufacturer's instructions of Human IL-8 (Thermo Fisher, 88-8086) and Human IL-6 (Thermo Fisher, 88-7066) kits as previously described (Ambrosio et al., 2023; Di Somma et al., 2019b). To normalize cytokine production, cells were detached with trypsin, centrifuged and

viable cells were counted using the trypan blue exclusion assay. Cytokine concentrations (pg/ml) were normalized and expressed as picograms per 10^6 viable cells.

2.7. Western blot

TNBC cells (6×10^4 cells) were cultured in 6-well plates with SAHA (at IC_{25} and IC_{50}) alone or in combination with the SOCS3 peptidomimetic KIRCONG chim PEG (15 μM) for 72h. After the treatments, cells were lysed in R.I.P.A. buffer (50 mM TRIS-HCl, pH 7.4, containing 150 mM NaCl, 0.5 M EDTA, 1 % NP-40, 0.5 % sodium deoxycholate, 0.1 % SDS) supplemented with phosphatase and protease inhibitors (1:100) and centrifuged at 17,000 g for 20 min at 4 °C, while cell culture supernatants were collected and stored at −80 °C for T cell activation assays. Protein concentration was quantified by Bradford Protein Assay (Bio-Rad, Berkeley, CA, USA). Equal amount of protein (30 μg) was diluted in Laemmli sample buffer and separated by SDS-PAGE as previously described (Malfitano et al., 2008). Proteins were resolved at a constant voltage of 100 mA and transferred onto 0,45 μm nitrocellulose blotting membrane (AmershamTM ProtranTM). Membranes were blocked in 5% non-fat dry milk in phosphate-buffered saline (PBS) containing 0.01% Tween-20 at R.T. for 1 h. Membranes were incubated overnight at 4 °C with anti-BAK (1:1000, Santa Cruz Biotechnology, sc-832), anti-phospho-STAT3 (Tyr705, 1:1000, R&D System, AF4607), anti-STAT3 (1:1000, R&D System, MAB1799), anti-SOCS3 (1:5000, 66797, Proteintech), anti-COX-2 (1:1000, PA5-17614, Invitrogen), anti-β actin mouse monoclonal IgG (1:2000, SC47778, Santa Cruz Biotechnology), anti-vinculin (1:2000, Santa Cruz Biotechnology, sc-73614), and anti-tubulin (1:10000, Sigma Aldrich, T9026).

Subsequently, membranes were incubated with the secondary antibodies for 1h at R.T. with the secondary antibody Goat anti-Rabbit IgG (H + L)-HRP conjugate (Cat. Num. 170-6515, Bio-Rad Laboratories, USA) for BAK and pSTAT3, and COX-2; and Goat anti-Mouse IgG (H + L)-HRP conjugate (Cat. Num. 170-6516, Bio-Rad Laboratories, USA) for STAT3, SOCS3, β-actin, vinculin, and tubulin. Protein bands were visualized using an enhanced chemiluminescence (ECL) system (Thermo Scientific, Rockford, IL, USA) as previously described (Napolitano et al., 2022; Moraca et al., 2025). Densitometric analysis was performed using Image Lab software version 3.0 (Bio-Rad, Hercules, CA, USA).

2.8. T cell activation assays

Conditioned media (CM) were collected from cells treated with SAHA alone at IC_{25} and IC_{50}, or in combination with KIRCONG chim PEG (15 μM). After 72 h of treatment, CM were harvested and centrifuged at 1600 g for 5 min to remove cell debris and stored at −80 °C until use. Freshly isolated PBMCs ($1x10^6$ cells/ml) from female healthy donors, were incubated with a 1:1 mixture of CM and fresh culture medium for 48 h h at 37 °C in a humidified atmosphere containing 5% CO_2. Phytohemagglutinin (PHA, 1:25, TCL071, HiMedia) was used as a positive control for T cell activation as previously described (Ciaglia et al., 2017). After incubation, PBMCs were collected, washed with PBS, and stained for 10 min at 4 °C in the dark with fluorochrome-conjugated antibodies: CD4-FITC, CD8-APC, HLA-DR-PE and CD69-PE (Miltenyi Biotec) as previously described (Malfitano et al., 2013, 2016). Cells were then washed, resuspended in FACS buffer, and analyzed using a BD LSRFortessa flow cytometer. T cell activation was evaluated by assessing the expression of HLA-DR and CD69 within $CD4^+$ and $CD8^+$ T cell subsets.

2.9. Statistical analysis

Statistical analyses were performed using GraphPad Prism version 10.4. Differences among groups were evaluated by Analysis of Variance (ANOVA) where required corrected for multiple comparison tests or by parametric unpaired two-tailed T test with Welch's corrections for pairwise comparisons. For non-parametric data the Kruskal-Wallis test or mixed-effect analysis with Fisher's LSD post-hoc test for multiple comparisons were applied. P values < 0.05 were considered statistically significant.

3. Results

3.1. SAHA inhibits TNBC cell viability

The effect of SAHA on cell viability was evaluated in TNBC cell lines MDA-MB-231, MDA-MB-468, and DU4475. Dose-response experiments using increasing concentrations of SAHA (0.04-10 μM) revealed a comparable inhibitory effect across all three cell lines after 72h of treatment (Fig. 1). A statistically significant reduction in cell viability was observed in all models, with MDA-MB-231 and MDA-MB-468 cells showing significant inhibition already at lower concentrations and at their IC_{25}. IC_{25} and IC_{50} values were found to be similar among the three cell lines (Table 1). For subsequent ICD characterization, MDA-MB-231 and MDA-MB-468 cells were selected as representative models, as they displayed greater responsiveness at lower SAHA concentrations and exhibit multi-driver molecular features. In contrast, DU4475 cells, which are primarily driven by a BRAF V600E mutation (Ku et al., 2022), were considered less suitable for studying immunogenic responses. TNBC cells were treated with SAHA at the IC_{25} for ICD-related assays. This sub-lethal concentration allows the evaluation of ICD-specific cellular events without inducing excessive cytotoxicity, thereby preserving sufficient cell viability for accurate assessment of extracellular ATP release, surface CALR exposure, and intracellular HMGB1 levels.

3.2. SAHA induces ICD in MDA-MB-231 cells

The effects of SAHA at its IC_{25} were investigated in MDA-MB-231 and MDA-MB-468 cells to evaluate modulation of the three main hallmarks of ICD: extracellular ATP release, CALR surface exposure and HMGB1 levels. SAHA treatment significantly increased ATP release in MDA-MB-231 cells, whereas the increase in MDA-MB-468 cells was not statistically significant. (Fig. 2A). Similarly, both CALR cell surface exposure and intracellular HMGB1 levels were upregulated exclusively in MDA-MB-231 cells, while no significant changes were detected in MDA-MB-468 cells (Fig. 2B–C). Consistently, extracellular HMGB1 release was increased in MDA-MB-231 cells after SAHA treatment. In two independent experiments, HMGB1 levels were 6038 ± 1128 pg/10^6 cells in untreated cells and 7131 ± 752 pg/10^6 cells in SAHA treated cells, corresponding to an approximate 15% increase, in agreement with the intracellular HMGB1 detection.

3.3. SAHA induces IL-6 in MDA-MB-231 cells

To investigate potential changes in the tumor-associated secretome, we evaluated the secretion of the pleiotropic cytokine IL-6 and the pro-inflammatory chemokine IL-8 in TNBC cells following 24h of SAHA treatment at its IC_{25}. Cytokine levels were quantified by ELISA. We observed that SAHA significantly increased IL-6 secretion in MDA-MB-231 cells, while no significant changes were observed in MDA-MB-468 cells (Fig. 3A). In contrast, IL-8 secretion was not significantly affected by SAHA treatment in either cell line, as no modulation was detected compared to the supernatant of untreated control cells (Fig. 3B).

To determine whether the difference in IL-6 secretion at the basal levels between the two cell lines could be explained by different SOCS3 expression, SOCS3 protein levels were measured. As previously reported, SOCS3 is expressed at low levels in MDA-MB-231 cells (Kim et al., 2015), while we observed higher expression in MDA-MB-468 cells consistently with the lower IL-6 secretion observed in these cells (Fig. 3C).

To explore potential pro-tumorigenic mechanisms underlying IL-6 upregulation in SAHA-treated MDA-MB-231 cells, we evaluated COX-2

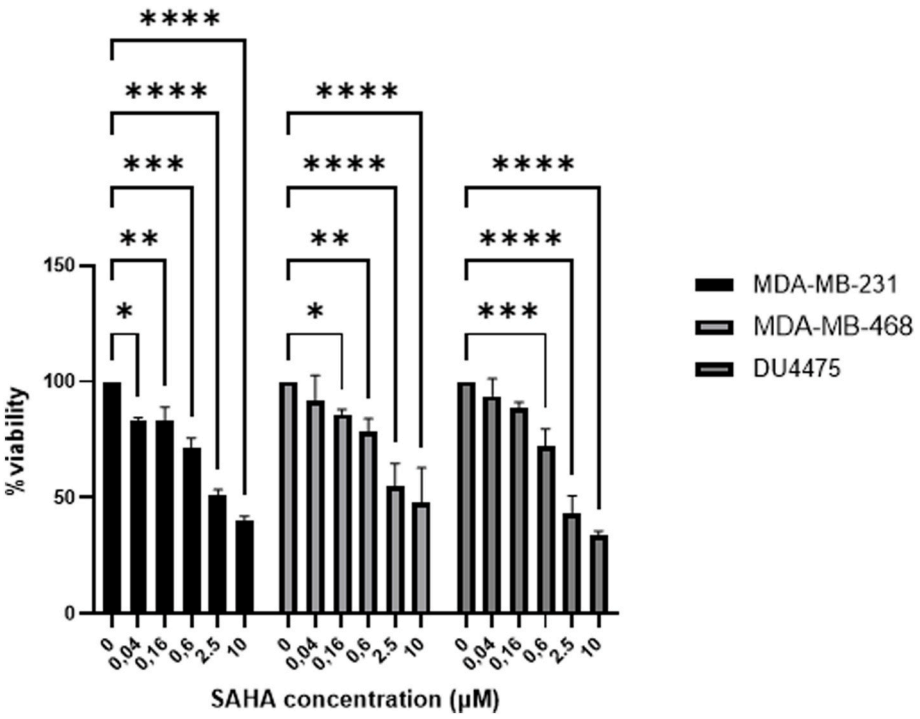

Fig. 1. SAHA inhibitory effect on cell viability. The effect of SAHA on MDA-MB-231, MDA-MB-468, and DU4475 was determined by MTT assay. Cell viability is expressed as percentage of survival relative to untreated control cells and histograms represent the mean ± SD of three independent experiments using increasing concentrations of SAHA. Statistical significance of cell survival inhibition versus untreated control cells was calculated by two-way ANOVA followed by Dunnett's multiple comparisons test (*$p < 0.05$, **$p < 0.01$, ***$p < 0.005$, ****$p < 0.0001$).

Table 1
IC25 and IC50 of SAHA in the investigated cell lines.

	MDA-MB-231	MDA-MB-468	DU4475
IC_{25}	0.25 ± 0.08	0.24 ± 0.12	0.32 ± 0.08
IC_{50}	0.91 ± 0.27	1.06 ± 0.84	0.94 ± 0.24

IC_{25} and IC_{50} (μM) values ± standard error (SEM) obtained for SAHA in MDA-MB-231 MDA-MB-468 and DU4475 cell lines after 72h of drug exposure. (IC_{25} values may differ from those reported in Section 3.5 as they derive from independent experiments).

expression, known to be upregulated in TNBC cells (Giunashvili et al., 2024) and to promote IL-6 induction via prostaglandin E2 (PGE2) (Pandey et al., 2024). A trend toward increased COX-2 expression was observed following SAHA treatment; however, this effect did not reach statistical significance (Supplemental Fig. S1).

The difference in IL-6 basal levels provides a mechanistic rationale for the use of the SOCS3 peptidomimetic KIRCONG chim PEG in MDA-MB-231 cells, aiming to functionally replace SOCS3 and inhibit IL-6/STAT3 signaling.

3.4. KIRCONG chim PEG in combination with SAHA decreases pSTAT3 expression and potentiates pro-apoptotic effects

To compensate for the low SOCS3 expression in MDA-MB-231 cells (Kim et al., 2015) and the increased IL-6 levels, SAHA at its IC_{25} and IC_{50} was combined with the SOCS3 peptidomimetic KIRCONG chim PEG (15 μM), designed to interact with JAK2 and inhibit pSTAT3 (Wang et al., 2024). The selected concentration of KIRCONG chim PEG was based on previous evidence demonstrating effective inhibition of STAT3 activation at low micromolar ranges. A PEG-modified SOCS3 mimetic has been reported to selectively penetrate TNBC cells and strongly inhibit STAT3 activation at comparable concentrations (La Manna et al., 2024). We therefore evaluated whether functional SOCS3 replacement could reduce pSTAT3 levels and enhance apoptosis in SAHA-treated cells. SAHA alone, at either IC_{25} or IC_{50}, did not significantly affect the pSTAT3/STAT3 ratio compared to untreated controls (Fig. 4). Notably, the combination of SAHA (IC_{25}) and KIRCONG chim PEG significantly reduced pSTAT3/STAT3 levels compared to SAHA alone (Fig. 4A). The combination of SAHA (IC_{50}) and KIRCONG chim PEG significantly reduced pSTAT3/STAT3 levels only compared to the untreated controls. As expected, KIRCONG chim PEG alone also decreased pSTAT3/STAT3 expression (Fig. 4).

To assess if the combinatory treatment enhanced apoptotic signaling, we evaluated the expression of the pro-apoptotic protein, BAK. SAHA alone increased BAK expression at both IC_{25} and IC_{50}, reaching a statistically significant effect only at the IC_{50} compared to untreated control cells (Fig. 4). At the IC_{25}, the effect of SAHA was significantly potentiated by KIRCONG chim PEG, with increased BAK expression compared to both untreated cells and single treatments. At IC_{50}, BAK levels remained higher in the combination compared to SAHA alone, however, statistical significance was reached only versus untreated controls and the peptidomimetic alone. Quantitatively, BAK expression (mean ± SEM) was 40.9 ± 8.5 in cell treated with SAHA (1 μM) alone and 70.1 ± 8.5 in cells treated with SAHA (1 μM) in combination with KIRCONG chim PEG (15 μM). The peptidomimetic alone did not exhibit pro-apoptotic effects (Fig. 4).

3.5. KIRCONG chim PEG enhances SAHA-induced cytotoxicity and T cell activation in MDA-MB-231 cells

To determine whether KIRCONG chim PEG potentiated SAHA-induced cytotoxicity, IC_{25} and IC_{50} values of SAHA were calculated in the presence or absence of the peptidomimetic (15 μM) by MTT assays. In MDA-MB-231 cells, co-treatment reduced the IC_{25} value from 0.22 ± 0.12 to 0.09 ± 0.05, while the IC_{50} remained unchanged. Although the reduction in IC_{25} did not reach statistical significance, it indicated a trend toward increased sensitivity to sub-toxic concentrations of SAHA.

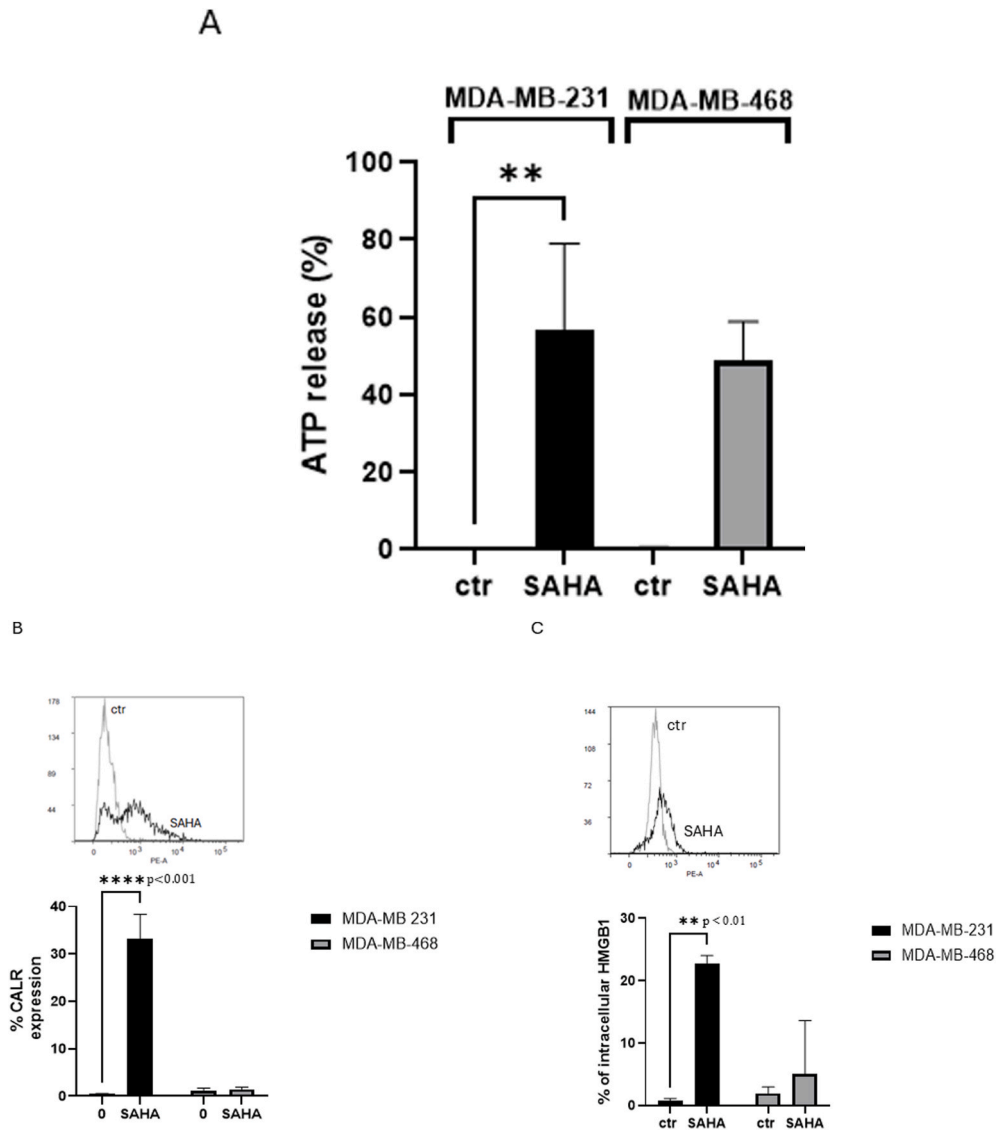

Fig. 2. SAHA induces ICD in MDA-MB-231 cells. TNBC cells were treated with SAHA at the IC_{25} for 72h to measure ICD markers: extracellular ATP release, CALR surface exposure, and intracellular HMGB1 levels. SAHA increased extracellular ATP release (A) in both MDA-MB-231 (black bars) and MDA-MB-468 (gray bars) cell lines, although statistical significance was reached only in MDA-MB-231 cells. SAHA upregulated CALR expression exclusively in MDA-MB-231 cells, as shown in the representative histogram and flowcytometric profile (B). Similarly, SAHA upregulated intracellular HMGB1 levels only in MDA-MB-231 cells (C). Data are representative of at least three independent experiments. Statistical analysis was performed by Kruskal-Wallis test (**p < 0.01, ***p < 0.001).

The peptidomimetic alone did not affect cell viability, supporting its role as a signaling modulator rather than a direct cytotoxic agent.

In contrast, in MDA-MB-468 cells, which display constitutive STAT3 phosphorylation (data not shown), the combination did not significantly modify SAHA-induced cytotoxicity.

To assess the functional immunological consequences of treatment, PBMC were incubated with conditioned media (CM) collected from MDA-MB-231 cells treated with SAHA alone or in combination with KIRCONG chim PEG. As a positive control for T cell activation, PBMC were stimulated with PHA. Expression of the activation markers HLA-DR and CD69 was assessed on $CD4^+$ and $CD8^+$ T cells. CM derived from co-treated tumor cells significantly increased HLA-DR and CD69 expression selectively in the $CD4^+$ T cell subset, whereas no significant modulation was observed in $CD8^+$ T cells (Fig. 5).

4. Discussion

In recent years numerous HDACi have been developed, and their promising anticancer efficacy has supported their advancement into clinical trials (Mann et al., 2007). However, although limited efficacy has been observed when using HDACi as single agents, they have been reported to enhance the sensitivity of BC cells to radiotherapy and chemotherapy (Chiu et al., 2013) and to exert synergic or additive effects when combined with conventional chemotherapeutic agents (Wawruszak et al., 2015). Based on these findings, we investigated the specific effects of SAHA in TNBC models using cell lines representative of distinct molecular subtypes.

Our results demonstrate that SAHA exerts a significant inhibitory effect on TNBC cell viability in MDA-MB-231, MDA-MB-468 and DU4475 cells, with comparable IC_{25} and IC_{50} values across the three models. Previous studies have reported the anti-proliferative effects of HDACi in TNBC cells (Nimal et al., 2025). In particular, SAHA was shown to inhibit proliferation in MDA-MB-231 and MDA-MB-468 cells after 48h of treatment with MDA-MB-468 cells appearing more resistant (Wawruszak et al., 2019). To better characterize the mechanisms underlying SAHA-mediated cytotoxicity and considering its reported immunomodulatory properties (Medon et al., 2017; Shen et al., 2017; Laengle et al., 2020), we selected more responsive MDA-MB-231 and

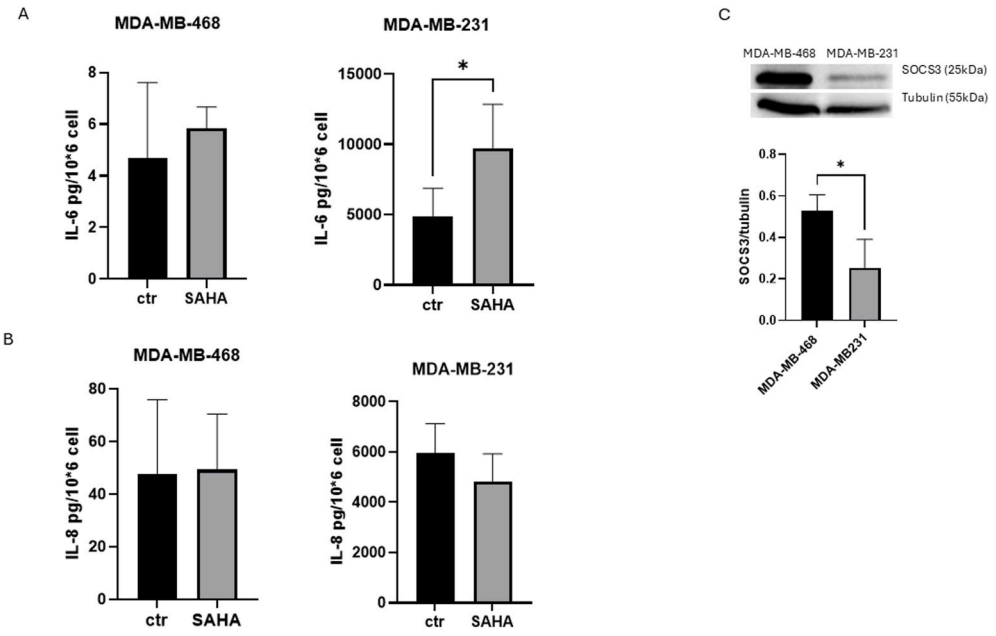

Fig. 3. SAHA affects cytokine secretion and basal SOCS3 levels in TNBC cells. TNBC cells were serum-starved overnight and then treated with SAHA at the IC_{25} for 24h. IL-6 (A) and IL-8 (B) secretion were measured in cell supernatants and normalized to the number of viable cells. Histograms are representative of three independent experiments. A statistically significant increase of IL-6 was detected in MDA-MB-231 cells. Basal SOCS3 protein expression in untreated MDA-MB-231 and MDA-MB-468 cells was evaluated by Western blot analysis. A representative immunoblot is reported. The densitometric quantification normalized to tubulin represents the mean ± SD of three independent tests, indicating lower SOCS3 expression in MDA-MB-231 cells compared to MDA-MB-468 cells (C). Statistical analysis was performed using unpaired *t*-test for densitometric analysis and with Welch's corrections for ELISA data (*p < 0.05).

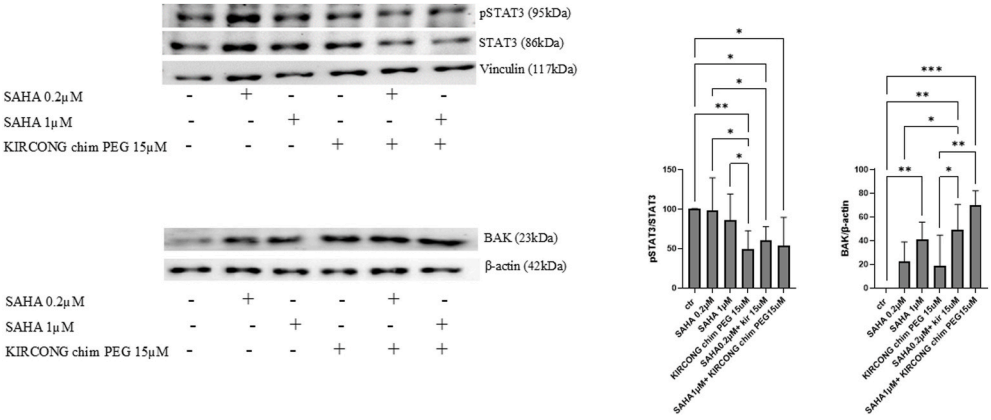

Fig. 4. Combinatory effect on pSTAT3 and BAK expressions. TNBC cells were treated with SAHA and KIRCONG chim PEG for 72h at the concentrations indicated. Protein expression levels of pSTAT3, STAT3, and BAK are shown. As control vinculin and β-actin were used. The reported densitometric analyses represent the mean ± SD of three independent experiments. Statistical analyses were performed by mixed-effect analysis with Fisher's LSD test post-hoc test for multiple comparisons. (*p < 0.05, **p < 0.01, ***p < 0.001).

MDA-MB-468 cells and evaluated key hallmarks of ICD, including extracellular ATP release, CALR surface exposure, and HMGB1intracellular levels and release (Di Somma et al., 2019b).

We selected the IC_{25} concentration for subsequent experiments, in agreement with previously published studies (Pang et al., 2023) and to avoid excessive cell death that could mask immunogenic signals and prevent discrimination between ICD-specific effects and general cytotoxicity. At IC_{25}, SAHA induced extracellular ATP release in both MDA-MB-231 and MDA-MB-468 cells, reaching statistical significance in MDA-MB-231 cells. However, CALR surface exposure and increased intracellular HMGB1 levels, together with detectable HMGB1 release, were observed exclusively in MDA-MB-231 cells. These findings indicate that SAHA induces full ICD in MDA-MB-231 cells, whereas MDA-MB-468 cells do not undergo complete ICD under the same conditions. This difference reflects intrinsic biological heterogeneity between the two TNBC models.

Afterwards, we evaluated modulation of secretome by measuring IL-6 and IL-8 levels. In particular, IL-6 is a key activator of the JAK/STAT3 pathway, promoting STAT3 phosphorylation and supporting cancer cell survival, proliferation, and immune modulation in TNBC (Malekinejad et al., 2025; Liu et al., 2023).

Notably, SAHA significantly upregulated IL-6 in MDA-MB-231 cells, without affecting IL-8 levels in either cell line. In addition, given the established role of COX-2 in promoting IL-6 production through prostaglandin E2 (PGE2) (Pandey et al., 2024), we observed a trend toward increased COX-2 expression following SAHA treatment, although not reaching statistical significance. This trend may be consistent with a contribution of COX-2-mediated inflammatory signaling to IL-6

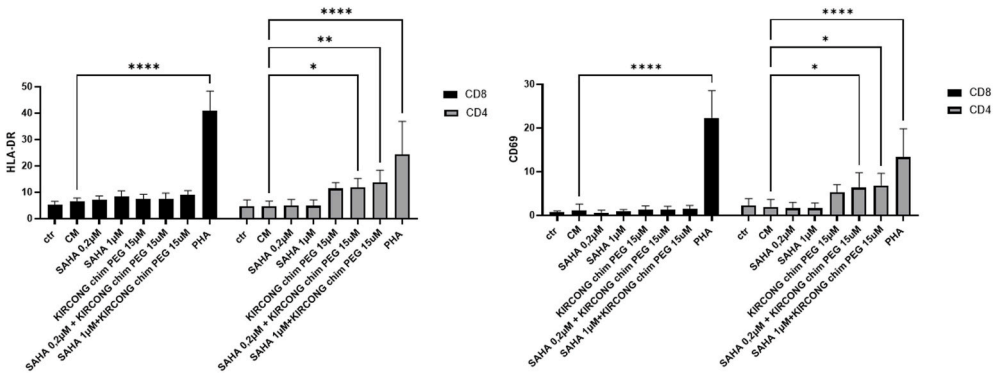

Fig. 5. Combinatory effect on T cell activation. CM collected from MDA-MB-231 cells treated with SAHA (IC_{25} and IC_{50}) in the presence or absence of KIRCONG chim PEG (15 μM) for 72h, was added to PBMC for 48h. Expression of the activation markers HLA-DR and CD69 was evaluated on $CD4^+$ and $CD8^+$ T cells by flow cytometry. PHA was used as a positive control for T activation. Data are representative of five independent experiments. Statistical analysis was performed by two-way ANOVA followed by Dunnett's multiple comparisons test (*$p < 0.05$, **$p < 0.01$, ****$p < 0.0001$).

upregulation. However, further studies would be required to clarify the mechanistic link between COX-2 modulation and IL-6 secretion in this setting. Although increased IL-6 and COX-2 are generally associated with pro-tumorigenic signaling, this effect appears to be counter-balanced by SAHA-reduced cell growth and ICD induction.

Moreover, MDA-MB-231 and MDA-MB-468 cells displayed distinct basal IL-6 secretion. The higher IL-6 secretion in MDA-MB-231 cells is consistent with their lower basal SOCS3 expression compared to MDA-MB-468 cells. Previous reports showed high basal IL-6 and low SOCS3 levels in MDA-MB-231 cells (Kim et al., 2015).

Despite exhibiting similar cytotoxic sensitivity to SAHA, MDA-MB-231 and MDA-MB-468 cells belong to distinct TNBC molecular subtypes. MDA-MB-231 cells display a claudin-low/EMT-like phenotype, whereas MDA-MB-468 cells are representative of a basal-like subtype with different signaling features. These intrinsic differences likely contribute to distinct immunogenic responses including ICD and IL-6 modulation, independently of overall cytotoxic sensitivity.

The up-regulation of IL-6 observed in MDA-MB-231 cells is consistent with reports suggesting that activation of the IL-6/JAK/STAT3 axis may limit HDACi efficacy (Liang et al., 2022). To address this possibility, we evaluated pSTAT3 expression in MDA-MB-231 cells treated with SAHA in combination with the SOCS3 peptidomimetic KIRCONG chim PEG (La Manna et al., 2024), given that SOCS3 is a physiological negative regulator of IL-6 signaling (Croker et al., 2003). Co-treatment reduced pSTAT3/STAT3 levels and increased expression of BAK, supporting that SOCS3 functional replacement enhances the anti-cancer activity of SAHA.

The improved anti-cancer effect with the combinatory treatment might be ascribed to a dual mechanism involving ICD induction and suppression of STAT3-dependent resistance pathways.

Consistently, co-treatment reduced the IC_{25} of SAHA in MDA-MB-231 cells, suggesting increased sensitivity to sub-toxic concentrations of HDAC inhibition. The absence of effect on IC_{50} may support the fact that this concentration already induces near-maximal cytotoxicity.

In contrast, IC_{25} and IC_{50} values were not significantly altered in MDA-MB-468 cells, supporting the context-dependent nature of SOCS3 replacement. Although STAT3 phosphorylation is detectable in MDA-MB-468 cells, their relatively low basal IL-6 levels suggest that STAT3 activation may be maintained by alternative signaling pathways independent of IL-6.

To explore the functional immunological relevance of SAHA-induced ICD, we evaluated T cell activation in response to CM from treated tumor cells. CM from MDA-MB-231 cells co-treated with SAHA and KIRCONG chim PEG significantly increased HLA-DR and CD69 expression selectively in $CD4^+$ T cells, whereas $CD8^+$ T cells were not significantly affected. The preferential activation of $CD4^+$ T cells is consistent with enhanced helper T cell priming, which plays a critical role in orchestrating anti-tumor immunity by supporting cytotoxic T lymphocyte expansion and shaping the tumor microenvironment. The lack of $CD8^+$ T cell activation may reflect the absence of direct antigen presentation in this in vitro system.

Importantly, enhanced $CD4^+$ T cell activation is consistent with the dual mechanism observed in MDA-MB-231 cells, in which induction of ICD is coupled with suppression of IL-6/STAT3-mediated inflammatory resistance. Thus, SOCS3 functional replacement appears not only to enhance cytotoxicity but also to amplify the immunogenic potential of HDAC inhibition in IL-6–high TNBC cells.

Compared with broad-spectrum chemotherapeutics or direct JAK inhibitors, this strategy represents a rational and selective approach targeting both tumor-intrinsic survival pathways and immune-regulatory circuits.

Overall, our findings demonstrate that coupling HDAC inhibition with targeted disruption of the IL-6/STAT3 axis enhances both cytotoxic and immunogenic responses in inflammatory TNBC models. Validation in immunocompetent in vivo systems will be necessary to determine the translational potential of this combinatory strategy and its impact on tumor–immune interactions within the tumor microenvironment.

CRediT authorship contribution statement

Giuliano Castellano: Methodology, Data curation. **Candida Bucciero:** Methodology, Data curation. **Alessia Cugudda:** Methodology, Data curation. **Sara La Manna:** Methodology, Data curation. **Daniela Marasco:** Validation, Funding acquisition. **Giuseppe Portella:** Visualization, Supervision. **Anna Maria Malfitano:** Writing – review & editing, Funding acquisition, Conceptualization.

Funding sources

This work was supported by: PROGETTI DI RICERCA DI RILEVANTE INTERESSE NAZIONALE (PRIN) 000013_PRIN_2022_(Malfitano_A.M.) cod.20224JSC3M, and by Associazione Italiana per la Ricerca sul Cancro (AIRC) grant IG 2022, cod. 27378 (Marasco D.).

Declaration of competing interest

The authors declare that they have no known competing financial interests or personal relationships that could have appeared to influence the work reported in this paper.

Acknowledgements

We thank Dr. Leonardo Cristinziano for helpful technical assistance.

Appendix A. Supplementary data

Supplementary data to this article can be found online at https://doi.org/10.1016/j.ejphar.2026.178960.

Data availability

row data are provided in supplementary material.

References

Ambrosio, M.R., Migliaccio, T., Napolitano, F., Di Somma, S., Maneli, G., Amato, J., Pagano, B., Randazzo, A., Portella, G., Formisano, P., Malfitano, A.M., 2023. Targeting G-quadruplex motifs interferes with differentiation of adipose-derived mesenchymal stem cells. Stem Cell Res. Ther. 14, 98.

Bianchini, G., De Angelis, C., Licata, L., Gianni, L., 2022. Treatment landscape of triple-negative breast cancer - expanded options, evolving needs. Nat. Rev. Clin. Oncol. 19, 91–113.

Bolden, J.E., Shi, W., Jankowski, K., Kan, C.Y., Cluse, L., Martin, B.P., Mackenzie, K.L., Smyth, G.K., Johnstone, R.W., 2013. HDAC inhibitors induce tumor-cell-selective pro-apoptotic transcriptional responses. Cell Death Dis. 4, e519.

Chiu, H.W., Yeh, Y.L., Wang, Y.C., Huang, W.J., Chen, Y.A., Chiou, Y.S., Ho, S.Y., Lin, P., Wang, Y.J., 2013. Suberoylanilide hydroxamic acid, an inhibitor of histone deacetylase, enhances radiosensitivity and suppresses lung metastasis in breast cancer in vitro and in vivo. PLoS One 8, e76340.

Ciaglia, E., Malfitano, A.M., Laezza, C., Fontana, A., Nuzzo, G., Cutignano, A., Abate, M., Pelin, M., Sosa, S., Bifulco, M., Gazzerro, P., 2017. Immuno-modulatory and anti-inflammatory effects of dihydrogracilin A, a terpene derived from the marine sponge Dendrilla membranosa. Int. J. Mol. Sci. 18.

Croker, B.A., Krebs, D.L., Zhang, J.G., Wormald, S., Willson, T.A., Stanley, E.G., Robb, L., Greenhalgh, C.J., Förster, I., Clausen, B.E., Nicola, N.A., Metcalf, D., Hilton, D.J., Roberts, A.W., Alexander, W.S., 2003. SOCS3 negatively regulates IL-6 signaling in vivo. Nat. Immunol. 4, 540–545.

Di Somma, S., Amato, J., Iaccarino, N., Pagano, B., Randazzo, A., Portella, G., Malfitano, A.M., 2019a. G-Quadruplex binders induce immunogenic cell death markers in aggressive breast cancer cells. Cancers (Basel) 11.

Di Somma, S., Iannuzzi, C.A., Passaro, C., Forte, I.M., Iannone, R., Gigantino, V., Indovina, P., Botti, G., Giordano, A., Formisano, P., Portella, G., Malfitano, A.M., Pentimalli, F., 2019b. The oncolytic virus dl922-947 triggers immunogenic cell death in mesothelioma and reduces xenograft growth. Front. Oncol. 9, 564.

Florio, D., Malfitano, A.M., Di Somma, S., Mügge, C., Weigand, W., Ferraro, G., Iacobucci, I., Monti, M., Morelli, G., Merlino, A., Marasco, D., 2019. Platinum(II) O,S complexes inhibit the aggregation of amyloid model systems. Int. J. Mol. Sci. 20.

Gameiro, S.R., Malamas, A.S., Tsang, K.Y., Ferrone, S., Hodge, J.W., 2016. Inhibitors of histone deacetylase 1 reverse the immune evasion phenotype to enhance T-cell mediated lysis of prostate and breast carcinoma cells. Oncotarget 7, 7390–7402.

Giannini, G., Cabri, W., Fattorusso, C., Rodriquez, M., 2012. Histone deacetylase inhibitors in the treatment of cancer: overview and perspectives. Future Med. Chem. 4, 1439–1460.

Giunashvili, N., Thomas, J.M., Schvarcz, C.A., Viana, P.H.L., Aloss, K., Bokhari, S.M.Z., Koós, Z., Bócsi, D., Major, E., Balogh, A., Benyó, Z., Hamar, P., 2024. Enhancing therapeutic efficacy in triple-negative breast cancer and melanoma: synergistic effects of modulated electro-hyperthermia (mEHT) with NSAIDs especially COX-2 inhibition in in vivo models. Mol. Oncol. 18, 1012–1030.

Göttlicher, M., Minucci, S., Zhu, P., Krämer, O.H., Schimpf, A., Giavara, S., Sleeman, J.P., Lo Coco, F., Nervi, C., Pelicci, P.G., Heinzel, T., 2001. Valproic acid defines a novel class of HDAC inhibitors inducing differentiation of transformed cells. Embo j 20, 6969–6978.

He, L.Z., Tolentino, T., Grayson, P., Zhong, S., Warrell Jr., R.P., Rifkind, R.A., Marks, P. A., Richon, V.M., Pandolfi, P.P., 2001. Histone deacetylase inhibitors induce remission in transgenic models of therapy-resistant acute promyelocytic leukemia. J. Clin. Investig. 108, 1321–1330.

Huang, Z., Zhou, W., Li, Y., Cao, M., Wang, T., Ma, Y., Guo, Q., Wang, X., Zhang, C., Zhang, C., Shen, W., Liu, Y., Chen, Y., Zheng, J., Yang, S., Fan, Y., Xiang, R., 2018. Novel hybrid molecule overcomes the limited response of solid tumours to HDAC inhibitors via suppressing JAK1-STAT3-BCL2 signalling. Theranostics 8, 4995–5011.

Jiang, X.C., Tu, F.H., Wei, L.Y., Wang, B.Z., Yuan, H., Yuan, J.M., Rao, Y., Huang, S.L., Li, Q.J., Ou, T.M., Wang, H.G., Tan, J.H., Chen, S.B., Huang, Z.S., 2022. Discovery of a novel G-Quadruplex and histone deacetylase (HDAC) dual-targeting agent for the treatment of triple-negative breast cancer. J. Med. Chem. 65, 12346–12366.

Kelly, W.K., O'connor, O.A., Krug, L.M., Chiao, J.H., Heaney, M., Curley, T., Macgregore-Cortelli, B., Tong, W., Secrist, J.P., Schwartz, L., Richardson, S., Chu, E., Olgac, S., Marks, P.A., Scher, H., Richon, V.M., 2005. Phase I study of an oral histone deacetylase inhibitor, suberoylanilide hydroxamic acid, in patients with advanced cancer. J. Clin. Oncol. 23, 3923–3931.

Kim, G., Ouzounova, M., Quraishi, A.A., Davis, A., Tawakkol, N., Clouthier, S.G., Malik, F., Paulson, A.K., D'angelo, R.C., Korkaya, S., Baker, T.L., Esen, E.S., Prat, A., Liu, S., Kleer, C.G., Thomas, D.G., Wicha, M.S., Korkaya, H., 2015. SOCS3-mediated regulation of inflammatory cytokines in PTEN and p53 inactivated triple negative breast cancer model. Oncogene 34, 671–680.

Ku, G.C., Chapdelaine, A.G., Ayrapetov, M.K., Sun, G., 2022. Identification of lethal inhibitors and inhibitor combinations for mono-driver versus multi-driver triple-negative breast cancer cells. Cancers (Basel) 14.

La Manna, S., Cugudda, A., Mercurio, F.A., Leone, M., Fortuna, S., Di Natale, C., Lagreca, E., Netti, P.A., Panzetta, V., Marasco, D., 2024. PEGylated SOCS3 mimetics encapsulated into PLGA-NPs as selective inhibitors of JAK/STAT pathway in TNBC cells. Int. J. Nanomed. 19, 7237–7251.

La Manna, S., Roviello, V., Napolitano, F., Malfitano, A.M., Monaco, V., Merlino, A., Monti, M., Kowalski, K., Szczupak, Ł., Marasco, D., 2023. Metal-complexes bearing releasable CO differently modulate amyloid aggregation. Inorg. Chem. 62, 10470–10480.

Laengle, J., Kabiljo, J., Hunter, L., Homola, J., Prodinger, S., Egger, G., Bergmann, M., 2020. Histone deacetylase inhibitors valproic acid and vorinostat enhance trastuzumab-mediated antibody-dependent cell-mediated phagocytosis. J. Immunother. Cancer 8.

Li, M., Viswanadhapalli, S., Santhamma, B., Pratap, U.P., Luo, Y., Liu, J., Altwegg, K.A., Tang, W., Liu, Z., Li, X., Ebrahimi, B., Yan, H., Zou, Y., Konda, S., Sareddy, G.R., Xu, Z., Chen, Y., Rao, M.K., Brenner, A.J., Kaklamani, V.G., Tekmal, R.R., Ahmed, G., Raj, G.V., Nickisch, K.J., Nair, H.B., Vadlamudi, R.K., 2021. LIFR inhibition enhances the therapeutic efficacy of HDAC inhibitors in triple negative breast cancer. Commun. Biol. 4, 1235.

Liang, X., Tang, S., Liu, X., Liu, Y., Xu, Q., Wang, X., Saidahmatov, A., Li, C., Wang, J., Zhou, Y., Zhang, Y., Geng, M., Huang, M., Liu, H., 2022. Discovery of novel Pyrrolo [2,3-d]pyrimidine-based derivatives as potent JAK/HDAC dual inhibitors for the treatment of refractory solid tumors. J. Med. Chem. 65, 1243–1264.

Liu, H., Yan, R., Xiao, Z., Huang, X., Yao, J., Liu, J., An, G., Ge, Y., 2023. Targeting DCLK1 attenuates tumor stemness and evokes antitumor immunity in triple-negative breast cancer by inhibiting IL-6/STAT3 signaling. Breast Cancer Res. 25, 43.

Malekinejad, Z., Aghdam, E.M., Ardakan, A.K., Forghan, E., Alizadeh, M., Simiyari, R., Heidari, H.R., Montazersaheb, S., 2025. Targeting STAT3 pathway: a promising immunotherapeutic strategy for triple-negative breast cancer - current status and future outlooks. Eur. J. Pharmacol. 1005, 178079.

Malfitano, A.M., Laezza, C., D'alessandro, A., Procaccini, C., Saccomanni, G., Tuccinardi, T., Manera, C., Macchia, M., Matarese, G., Gazzerro, P., Bifulco, M., 2013. Effects on immune cells of a new 1,8-naphthyridin-2-one derivative and its analogues as selective CB2 agonists: implications in multiple sclerosis. PLoS One 8, e62511.

Malfitano, A.M., Laezza, C., Pisanti, S., Gazzerro, P., Bifulco, M., 2008. Rimonabant (SR141716) exerts anti-proliferative and immunomodulatory effects in human peripheral blood mononuclear cells. Br. J. Pharmacol. 153, 1003–1010.

Malfitano, A.M., Laezza, C., Pisanti, S., Manera, C., Bifulco, M., 2016. Immuno-modulatory properties of a Quinolin-2-(1H)-on-3-Carboxamide derivative: relevance in multiple sclerosis. Recent Pat. CNS Drug Discov. 10, 113–121.

Mann, B.S., Johnson, J.R., Cohen, M.H., Justice, R., Pazdur, R., 2007. FDA approval summary: vorinostat for treatment of advanced primary cutaneous T-cell lymphoma. Oncologist 12, 1247–1252.

Medon, M., Vidacs, E., Vervoort, S.J., Li, J., Jenkins, M.R., Ramsbottom, K.M., Trapani, J. A., Smyth, M.J., Darcy, P.K., Atadja, P.W., Henderson, M.A., Johnstone, R.W., Haynes, N.M., 2017. HDAC inhibitor panobinostat engages host innate immune defenses to promote the tumoricidal effects of trastuzumab in HER2(+) tumors. Cancer Res. 77, 2594–2606.

Min, A., Im, S.A., Kim, D.K., Song, S.H., Kim, H.J., Lee, K.H., Kim, T.Y., Han, S.W., Oh, D. Y., Kim, T.Y., O'connor, M.J., Bang, Y.J., 2015. Histone deacetylase inhibitor, suberoylanilide hydroxamic acid (SAHA), enhances anti-tumor effects of the poly (ADP-ribose) polymerase (PARP) inhibitor olaparib in triple-negative breast cancer cells. Breast Cancer Res. 17, 33.

Moraca, F., Arciuolo, V., Marzano, S., Napolitano, F., Castellano, G., D'aria, F., Di Porzio, A., Landolfi, L., Catalanotti, B., Randazzo, A., Pagano, B., Malfitano, A.M., Amato, J., 2025. Repurposing FDA-approved drugs to target G-quadruplexes in breast cancer. Eur. J. Med. Chem. 285, 117245.

Napolitano, F., Di Somma, S., Castellano, G., Amato, J., Pagano, B., Randazzo, A., Portella, G., Malfitano, A.M., 2022. Combination of dl922-947 oncolytic adenovirus and G-Quadruplex binders uncovers improved antitumor activity in breast cancer. Cells 11.

Nimal, S., Kumbhar, N., Pote, M.S., Bankar, R., Shaikh, M., Gacche, R., 2025. Reversal of epithelial to mesenchymal transition in triple negative breast cancer through epigenetic modulations by dietary flavonoid galangin and its combination with SAHA. Cell Commun. Signal. 23, 163.

Nimal, S., Kumbhar, N., Saruchi, Rathore, S., Naik, N., Paymal, S., Gacche, R.N., 2024. Apigenin and its combination with vorinostat induces apoptotic-mediated cell death in TNBC by modulating the epigenetic and apoptotic regulators and related miRNAs. Sci. Rep. 14, 9540.

Oba, T., Ono, M., Matoba, H., Uehara, T., Hasegawa, Y., Ito, K.I., 2021. HDAC6 inhibition enhances the anti-tumor effect of eribulin through tubulin acetylation in triple-negative breast cancer cells. Breast Cancer Res. Treat. 186, 37–51.

Pandey, V.K., Premkumar, K., Kundu, P., Shankar, B.S., 2024. PGE2 induced miR365/IL-6/STAT3 signaling mediates dendritic cell dysfunction in cancer. Life Sci. 350, 122751.

Pang, Y., Shi, R., Chan, L., Lu, Y., Zhu, D., Liu, T., Yan, M., Wang, Y., Wang, W., 2023. The combination of the HDAC1 inhibitor SAHA and doxorubicin has synergic efficacy in triple negative breast cancer in vivo. Pharmacol. Res. 196, 106926.

Shen, J., Pan, J., Du, C., Si, W., Yao, M., Xu, L., Zheng, H., Xu, M., Chen, D., Wang, S., Fu, P., Fan, W., 2017. Silencing NKG2D ligand-targeting miRNAs enhances natural killer cell-mediated cytotoxicity in breast cancer. Cell Death Dis. 8, e2740.

Terranova-Barberio, M., Thomas, S., Ali, N., Pawlowska, N., Park, J., Krings, G., Rosenblum, M.D., Budillon, A., Munster, P.N., 2017. HDAC inhibition potentiates immunotherapy in triple negative breast cancer. Oncotarget 8, 114156–114172.

Vasilatos, S.N., Katz, T.A., Oesterreich, S., Wan, Y., Davidson, N.E., Huang, Y., 2013. Crosstalk between lysine-specific demethylase 1 (LSD1) and histone deacetylases

mediates antineoplastic efficacy of HDAC inhibitors in human breast cancer cells. Carcinogenesis 34, 1196–1207.
Wang, T., Kaneko, S., Kriukov, E., Alvarez, D., Lam, E., Wang, Y., La Manna, S., Marasco, D., Fernandez-Gonzalez, A., Mitsialis, S.A., Kourembanas, S., Stahl, A., Chen, M., Xu, H., Baranov, P., Cai, G., Von Andrian, U.H., Sun, Y., 2024. SOCS3 regulates pathological retinal angiogenesis through modulating SPP1 expression in microglia and macrophages. Mol. Ther. 32, 1425–1444.
Wawruszak, A., Gumbarewicz, E., Okon, E., Jeleniewicz, W., Czapinski, J., Halasa, M., Okla, K., Smok-Kalwat, J., Bocian, A., Rivero-Muller, A., Stepulak, A., 2019. Histone deacetylase inhibitors reinforce the phenotypical markers of breast epithelial or mesenchymal cancer cells but inhibit their migratory properties. Cancer Manag. Res. 11, 8345–8358.
Wawruszak, A., Luszczki, J.J., Grabarska, A., Gumbarewicz, E., Dmoszynska-Graniczka, M., Polberg, K., Stepulak, A., 2015. Assessment of interactions between cisplatin and two histone deacetylase inhibitors in MCF7, T47D and MDA-MB-231 human breast cancer cell lines - an isobolographic analysis. PLoS One 10, e0143013.